

Hofstadter rules and generalized dimensions of the spectrum of Harper's equation

This article has been downloaded from IOPscience. Please scroll down to see the full text article.

1997 J. Phys. A: Math. Gen. 30 117

(<http://iopscience.iop.org/0305-4470/30/1/009>)

View [the table of contents for this issue](#), or go to the [journal homepage](#) for more

Download details:

IP Address: 171.66.16.71

The article was downloaded on 02/06/2010 at 04:18

Please note that [terms and conditions apply](#).

Hofstadter rules and generalized dimensions of the spectrum of Harper's equation

Andreas Rüdinger and Frédéric Piéchon

Institut für Theoretische und Angewandte Physik, Universität Stuttgart, Pfaffenwald 57, 70550 Stuttgart, Germany

Received 27 August 1996

Abstract. We consider the Harper model which describes two-dimensional Bloch electrons in a magnetic field. For irrational flux through the unit-cell the corresponding energy spectrum is known to be a Cantor set with multifractal properties. In order to relate the maximal and minimal fractal dimension of the spectrum of Harper's equation to the irrational number involved, we combine a refined version of the Hofstadter rules with results from semiclassical analysis and tunnelling in phase space. For quadratic irrationals ω with continued fraction expansion $\omega = [0; \bar{n}]$ the maximal fractal dimension exhibits oscillatory behaviour as a function of n , which can be explained by the structure of the renormalization flow. The asymptotic behaviour of the minimal fractal dimension is given by $\alpha_{\min} \sim \text{constant} \ln n/n$. As the generalized dimensions can be related to the anomalous diffusion exponents of an initially localized wavepacket, our results imply that the time evolution of high order moments $\langle r^q \rangle$, $q \rightarrow \infty$ is sensible to the parity of n .

0. Introduction

Originally conceived to describe Bloch electrons in a magnetic field [1], Harper's equation

$$\phi_{n+1} + \phi_{n-1} + 2 \cos(2\pi\omega n + \nu)\phi_n = E\phi_n \quad (1)$$

has become a subject of its own right. The parameter ω is the ratio between the magnetic flux per unit cell and the flux quantum, ϕ_n is related to the wavefunction of the Bloch electron and ν is a phase. Harper-like models are of great interest in a wide variety of physical contexts (integer quantum Hall effect [2], superconducting networks [3], electrons in superlattices [4]) and have given rise to strong interplay between physics and mathematics, as e.g. in the fields of semiclassics [5], non commutative geometry [6], and, quite recently, quantum groups [7]. Experimental investigations on superconducting networks permit a direct observation of the ground state energy as a function of the magnetic flux [3]. Furthermore, the resolution of the fine structure of Hofstadter's famous butterfly have been made possible by measuring the magnetoresistance oscillations in superlattices [4, 8].

During recent years there has been great interest in the generalized (Rényi) dimensions [9] of the spectral measure of this equation and similar quasiperiodic tight-binding Hamiltonians [10–17]. For the Harper equation it was conjectured that the fractal dimension $D_{q=0}$ is exactly $\frac{1}{2}$ for typical irrational numbers [15, 18]. Due to the Thouless property [19–21], however, there is a simple argument providing strong evidence for D_0 being

strictly smaller than $\frac{1}{2}$ [†]. Recently a statistical theory has been presented to explain the numerically observed behaviour of D_0 as a function of the irrational number $\omega = [0; \bar{n}]$ [22]. Until now there is no detailed investigation how the generalized dimensions D_q for a generic q depend on the incommensurability ω . However, the generalized dimensions play an important role for explaining the anomalous diffusion properties of wavepackets found in incommensurable models. Quite recently, the link between D_q and the anomalous diffusion $\langle r^q \rangle \sim t^{q\sigma_q}$ has been made explicit by the relation $\sigma_q = D_{1-q}$, which has been verified numerically [23].

In this paper we deal with the problem of the maximal and minimal fractal dimensions $\alpha_{\min} = D_{+\infty}$ and $\alpha^{\max} = D_{-\infty}$. This is intended to be a first step to general values of q . While α_{\min} (as D_0) exhibits a monotonic behaviour as a function of n , we find that α^{\max} shows strongly pronounced even-odd oscillations that can be explained by a refinement of the Hofstadter rules [26]. Similar behaviour of α_{\min} and α^{\max} has been found for a tight-binding Hamiltonian associated with substitution sequences using the trace map approach [24, 25].

The paper is organized as follows. We begin by reviewing the Hofstadter rules (1), then we consider the multifractal properties of Harper's equation for the case of the golden and silver mean (2) and finally pass to more general quadratic irrational numbers (3), where the minimal and maximal fractal dimensions of the related spectrum will be discussed in detail.

1. Hofstadter rules

The starting point of our considerations is the hierarchical clustering of the spectrum of Harper's equation (1). By inspecting the band structure of this equation as a function of ω , Hofstadter [26] noticed that for a given ω it consists of three parts, one central cluster (S) and two side clusters (R) that are closely related to the full spectra of Harper's equation with renormalized values of ω , namely $R(\omega)$ and $S(\omega)$ with

$$R(\omega) = \begin{cases} \left\{ \frac{1}{\omega} \right\} & \text{if } 0 < \omega < \frac{1}{2} \\ \left\{ \frac{1}{1-\omega} \right\} & \text{if } \frac{1}{2} < \omega < 1 \end{cases} \quad (2)$$

and

$$S(\omega) = \begin{cases} \left\{ \frac{\omega}{1-2\omega} \right\} & \text{if } 0 < \omega < \frac{1}{2} \\ \left\{ \frac{1-\omega}{2\omega-1} \right\} & \text{if } \frac{1}{2} < \omega < 1 \end{cases} \quad (3)$$

where $\{\cdot\}$ denotes the fractional part (for an illustration see [26, 18]).

These clustering rules, denoted as Hofstadter rules, have been derived afterwards by different methods [18, 28].

Until now, however, for practical calculations, it has always been assumed that the side clusters and the central cluster are simply rescaled versions of the full spectrum for the renormalized ω . Furthermore only the case of the golden and silver mean ($\omega_{\text{gold}} = [0; \bar{1}]$,

[†] Using, however, the thermodynamic formalism for the multifractal properties $\sum_{i=1}^N \Delta_j^{(1-q)D_q} \sim N^q$ [9], the Thouless property [19, 21, 20] for the scaling of the total bandwidth $\sum_{i=1}^N \Delta_j \sim N^{-1}$ gives immediately $D_{-1} = \frac{1}{2}$, and, therefore, $D_0 < D_{-1} = \frac{1}{2}$, provided D_q is strictly monotonically decreasing, that is the generic case for a multifractal.

$\omega_{\text{silver}} = [0; \bar{2}]$) has been considered. These particular values of ω are fixed points of both maps, R and S , and therefore self-consistent equations for the fractal dimension D_0 can be obtained easily [18].

In order to refine the assumption that the side and central clusters are merely homogeneously rescaled versions of the full spectrum for the renormalized ω , we rewrite Hofstadter's clustering rules in a more quantitative way. Consider the spectrum of a rational approximant $\omega = p/q$ with q bands. The partition of these bands on the lower side cluster, the central cluster and the upper side cluster is given according to $\text{den } \omega = q = \text{den } R(\omega) + \text{den } S(\omega) + \text{den } R(\omega)$, where 'den' denotes the denominator. Therefore we can write the q energy values E_i (upper or lower band edge, for large q , in which we are interested, the bandwidths go to zero, so there is no difference) in the following form [27]:

$$E_i(\omega) = \begin{cases} f_{\omega}^{-}(E_i(R(\omega))) & \text{for } i = 1, \dots, \text{den } R(\omega) \\ f_{\omega}^0(E_{i-\text{den } R(\omega)}(S(\omega))) & \text{for } i = \text{den } R(\omega) + 1, \dots, \text{den } R(\omega) \\ & + \text{den } S(\omega) \\ f_{\omega}^{+}(E_{i-\text{den } R(\omega)-\text{den } S(\omega)}(R(\omega))) & \text{for } i = \text{den } R(\omega) + \text{den } S(\omega) \\ & + 1, \dots, q. \end{cases} \quad (4)$$

The functions $f_{\omega}^{\pm,0}(E)$ are the fingerprints of Hofstadter's rules and are essential for calculating the fractal dimensions of the spectrum for a given ω . The irrational number ω can be developed in a continued fraction. Its truncation at the k th level yields the approximant of ω of generation k . An essential point is that $f_{\omega}^{\pm,0}(E)$ only depend weakly on the generation of the approximant of ω .

For a quasiperiodic tight-binding model where the Hofstadter rules also apply, the functions $f_{\omega}^{\pm,0}(E)$ have been calculated in a linear approximation by means of a renormalization approach for the case of the golden mean. Since ω_{gold} is invariant under S and R , the Hofstadter rules close up after the first step, leading to a self-consistent equation for the fractal dimensions [16].

A generic quadratic irrational number is not invariant under R and S , but successive applications of R and/or S involve a finite number of different irrational numbers. This can be seen, if the renormalization equations for ω are rewritten for the continued fraction expansion $\omega = [0; a_1, a_2, \dots]$:

$$R(\omega) = \begin{cases} [0; a_2, a_3, a_4, \dots] & \text{if } a_1 > 1 \\ [0; a_3, a_4, a_5, \dots] & \text{if } a_1 = 1 \end{cases} \quad (5)$$

and

$$S(\omega) = \begin{cases} [0; a_1 - 2, a_2, a_3, \dots] & \text{if } a_1 > 2 \\ [0; a_3, a_4, a_5, \dots] & \text{if } a_1 = 2 \\ [0; a_2 - 1, a_3, a_4, \dots] & \text{if } a_1 = 1, a_2 > 1 \\ [0; a_4, a_5, a_6, \dots] & \text{if } a_1 = 1, a_2 = 1. \end{cases} \quad (6)$$

Since quadratic numbers have periodic continued fraction expansions, only a finite number of different irrationals will occur by applying iteratively R and S to ω . Thus, once the functions $f_{\omega}(E)$ are known for all ω involved in the renormalization flow of the initial ω , the multifractal properties of the spectrum are determined.

We will restrict ourselves to quadratic numbers of the form $\omega = [0; \bar{n}]$. Examples of the renormalization flow are given in the following schematic representation for $n = 3, 4$:

	elementary cycles C	generation loss $d(C)$
n even	$S^j R, \quad 0 \leq j \leq \frac{1}{2}n - 1$	1
	$S^{n/2}$	2
n odd	$S^j R, \quad 0 \leq j \leq \frac{1}{2}(n-3)$	1
	$S^j R, \quad \frac{1}{2}(n-1) \leq j \leq n-1$	2
	S^n	3

Figure 1. Cycles occurring in the discrete renormalization diagram for $\omega = [0; \bar{n}]$.

The structure of these diagrams depends on the parity of n . For n odd, there are n irrational numbers involved and $n + 1$ cycles occur, n being of the form $S^j R$ and one of the form S^n . For n even, there are $n/2$ irrationals and $n/2$ cycles occur, $n/2 - 1$ of the form $S^j R$ and one of the form $S^{n/2}$.

Both of these cycles only leave invariant the exact irrational number ω . Applied to an approximant of ω of generation k , an approximant of ω , but of lower generation $k' < k$ is obtained, as is immediately obvious by inspecting (5) and (6). Thus, we can assign to each cycle a ‘generation loss’ $d := k - k'$ (cf figure 1).

2. Golden and silver number

For the sake of simplicity, we will begin by dealing with the problem for the case $\omega = \omega_{\text{gold, silver}}$, which are fixed points of the Hofstadter rules. The mapping $f_{\omega}^{\pm, 0}(E)$ has two different fixed points, denoted as **R** and **S** in figure 2, which correspond to the edges respectively to the centre of the spectrum. Assuming in a first approximation that the scaling properties of the spectrum are well described by the contraction factors at the centres and at the edges, $z_S = -\frac{df^0}{dE}|_{\text{centre}}$ and $z_R = \frac{df^{\pm}}{dE}|_{\text{edges}}$, we find that after k steps of renormalization, the bandwidths scale with $\Delta \sim z^k$ while the system size scales with $N \sim \tilde{\omega}^{-k \cdot d}$, where $\tilde{\omega}$ is the algebraically conjugate to ω ($\tilde{\omega} = \frac{1}{2}(n + \sqrt{n^2 + 4})$ for $\omega = [0; \bar{n}] = \frac{1}{2}(-n + \sqrt{n^2 + 4})$).

With $\Delta \sim N^{-1/\alpha}$ we obtain the two local scaling exponents at the edges and the centre of the band:

$$\alpha_S = -\frac{d(S) \ln \tilde{\omega}}{\ln z_S} \quad (7)$$

and

$$\alpha_R = -\frac{d(R) \ln \tilde{\omega}}{\ln z_R} \quad (8)$$

where $d(S)$ and $d(R)$ are the generation losses of the cycles R and S .

Furthermore, within this approximation a self-consistent equation for $\tau(q) = (q-1)D_q$, the Legendre transform of $f(\alpha)$, can be given directly:

$$\frac{2\omega^{d(R)q}}{z_R^{\tau}} + \frac{\omega^{d(S)q}}{z_S^{\tau}} = 1 \quad \omega = \omega_{\text{gold}}, \omega_{\text{silver}}. \quad (9)$$

For the case of the golden number, this equation has recently been used to derive the multifractal properties of a tight-binding Hamiltonian associated with the Fibonacci sequence in the limit of strong modulation [16]. Despite of being a good first approximation, the corresponding $f(\alpha)$ has two serious drawbacks: First, $f(\alpha_{\min})$ or $f(\alpha^{\max})$ (depending on the parameter) does not vanish in contradiction to numerical simulations and indications from the trace map approach [12]. This problem is due to the oversimplification of $f^{\pm, 0}$ by

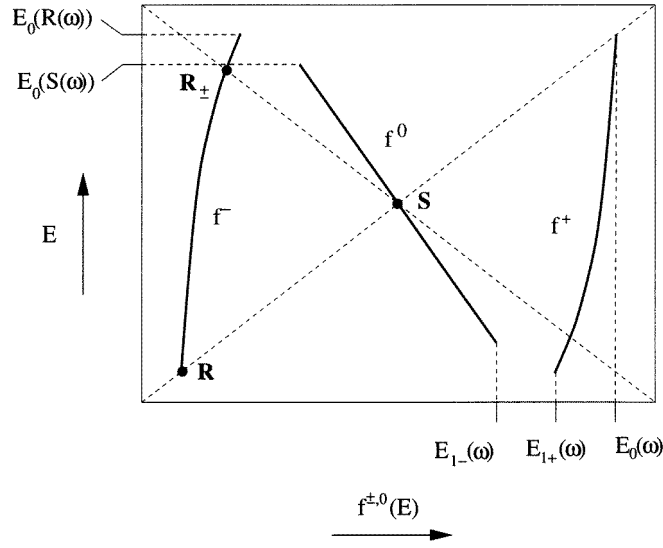


Figure 2. Schematic representation of $f^{\pm,0}(E)$. The points **R** and **S** are the fixed points of $f^{\pm,0}(E)$. The point **R**_± corresponds to the two-orbit $E \rightarrow -E \rightarrow E$.

three linear pieces, yielding an artificial degeneration of the widths of the bands (2^n bands of $\tilde{\omega}^n$ ones have the same widths), which leads to $f(\alpha_R) \neq 0$.

Second, in this approach the extremal scaling properties are found at the band edges or at the centre of the spectrum. This is, however, by far not the general case. It is true for ω_{gold} for both the Harper model and the quasiperiodic Hamiltonian mentioned above, but neither for ω_{silver} , nor for higher irrational numbers $\omega = [0; \bar{n}]$, $n \geq 3$.

In order to construct an approach eliminating these two problems, we consider the mapping of the spectrum by the renormalization flow as a discrete dynamical system. For ω_{gold} and ω_{silver} the spectral measure is given by the invariant measure of the map $f_{\omega}^{\pm,0}(E)$. The band edges and the band centre are attracting fixed points of $f_{\omega}^{\pm,0}(E)$, thus giving rise to nontrivial scaling behaviour, as we have seen above. To get accurate approximations of the $f(\alpha)$ -curves, however, we have to take into account higher periodic orbits of the underlying dynamical systems. The simplest approximation is to include the orbit R_+R_- of period two. The energies of the two (symmetric) fixed points are given by $f^{\pm}(E) = -E$. Therefore we find for the corresponding scaling factor

$$\alpha_{R_+R_-} = -\frac{d(R_+R_-) \ln \tilde{\omega}}{\ln z_{R_+} + \ln z_{R_-}} = -\frac{d(R) \ln \tilde{\omega}}{\ln z_{R_{\pm}}} \quad (10)$$

where $z_{R_{\pm}}$ is the local contraction factor at the fixed points of order two:

$$z_{R_{\pm}} = \left. \frac{df^{\pm,0}(E)}{dE} \right|_{E=-f^{\pm}(E)}. \quad (11)$$

Taking into account the three contraction factors $z_R, z_S, z_{R_{\pm}}$ (denoted as 3z-model in the following) we arrive at the following self-consistent equation for $\tau(q)$:

$$\frac{\omega^{d(R)q}}{z_R^{\tau}} + \frac{\omega^{d(R)q}}{z_{R_{\pm}}^{\tau}} + \frac{\omega^{d(S)q}}{z_S^{\tau}} = 1 \quad \omega = \omega_{\text{gold}}, \omega_{\text{silver}}. \quad (12)$$

If $z_{R_{\pm}}$ equals z_R equation (12) reduces to (9).

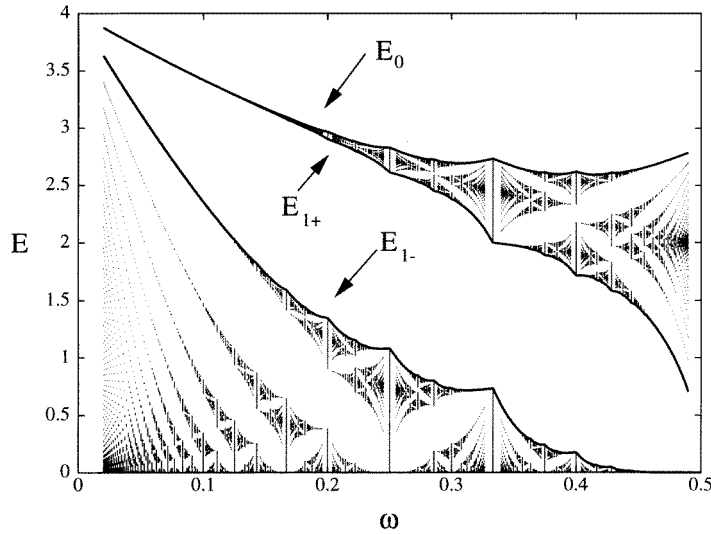


Figure 3. One quarter of the Hofstadter's butterfly. The band edges $E_0(\omega)$, $E_{1+}(\omega)$ and $E_{1-}(\omega)$ are depicted with lines.

The minimal and maximal dimensions for the $3z$ -model are given by $\alpha_{\min(\max)} = \min(\max)\{\alpha_R, \alpha_S, \alpha_{R\pm}\}$. By performing the Legendre transformation of (12) we find the correct behaviour $f(\alpha_{\min, \max}) = 0$. While for the golden number $\alpha^{\max} = \alpha_S > \alpha_{R\pm} > \alpha_R = \alpha_{\min}$, i.e. the maximal scaling exponent occurs at the centre of the spectrum, for the silver number the maximal dimension is given by $\alpha^{\max} = \alpha_{R\pm} > \alpha_S > \alpha_R = \alpha_{\min}$, i.e. the bands of maximal widths are not at the centre of the spectrum, but at the energy given by $f^\pm(E) = -E$. Therefore a linear approximation of $f_\omega^{\pm,0}(E)$ (i.e. two scaling factors, one for the central, and one for the side bands) is not sufficient for explaining α_{\min} and α^{\max} , even in the case of ω_{silver} .

The approximative $f(\alpha)$ -curves calculated from equation (12) are compared in figure 4 with those obtained by the usual multifractal formalism [9]. Despite of the simplicity of our model there is a good agreement between the curves. Including linearization around further periodic orbits of the nonlinear map $f^{\pm,0}(E)$ would yield further quantitative improvement. We consider the $3z$ -model as the simplest qualitatively correct approximation.

Let us note that the Thouless property $D_{-1} = \frac{1}{2}$ (i.e. $\tau(-1) = -1$) yields one linear equation which the three contraction factors have to fulfill:

$$\frac{z_R}{\omega^{d(R)}} + \frac{z_{R\pm}}{\omega^{d(R)}} + \frac{z_S}{\omega^{d(S)}} = 1 \quad \omega = \omega_{\text{gold}}, \omega_{\text{silver}}. \quad (13)$$

Thus, by use of this relation, the calculation of the scaling behaviour at the band-edges z_R and at the centre of the band z_S would enable us to obtain the missing contraction factor $z_{R\pm}$.

3. Higher quadratic irrational numbers

Hitherto we have been considering the case of the fixed points of the Hofstadter rules, where the renormalization always yields the same function $f_{R(\omega)}^{\pm,0}(E) = f_{S(\omega)}^{\pm,0}(E) = f_\omega^{\pm,0}(E)$ that can be considered as a dynamical system. We have shown that taking into account not only the fixed points of this dynamical system, but also a periodic orbit of length two,

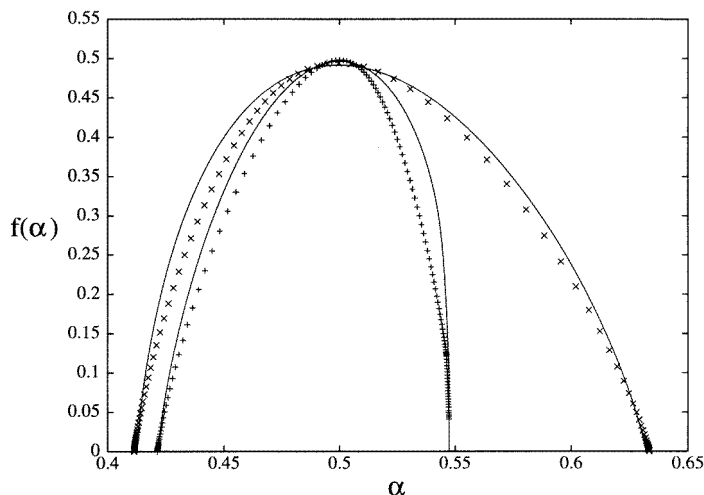


Figure 4. The multifractal spectrum $f(\alpha)$ for the Harper model for ω_{gold} (narrow curve) and ω_{silver} (large curve) compared to the $3z$ -model. The $f(\alpha)$ -curves obtained from diagonalization and the thermodynamic formalism are drawn with symbols, the $f(\alpha)$ obtained from Legendre-Transformation of (12) are depicted with lines ($z_R^{\text{gold}} = 0.103$, $z_{R\pm}^{\text{gold}} = 0.164$, $z_S^{\text{gold}} = 0.0718$; $z_R^{\text{silver}} = 0.118$, $z_{R\pm}^{\text{silver}} = 0.248$, $z_S^{\text{silver}} = 0.020$).

satisfactory $f(\alpha)$ -curves can be obtained. Now we generalize this approach to the irrational numbers $[0; \bar{n}]$ that are not fixed points of the Hofstadter rules but give rise to a nontrivial cycle structure that has been shown above.

In this case we have to deal not only with one function $f_{\omega}^{\pm,0}(E)$ but with a whole set of function $\{f_{\omega_i}^{\pm,0}(E)\}$, where the ω_i are the irrational numbers occurring in the flow diagram of ω . In order to calculate the scaling properties of the spectrum, we have to consider the cycles of the flow diagram. To each cycle there is one effective $f_{\text{eff}}^{\pm,0}(E)$ that results from concatenating the corresponding maps $f_{\omega_i}^{\pm,0}(E)$ for the ω_i occurring in this cycle. For example, the effective map of the cycle S^2R in the case of $\omega = [0; \bar{3}]$ is given by $f_{\text{eff}}^{\pm} = f_{[0;2;\bar{3}]}^{\pm} \circ f_{[0;1;\bar{3}]}^0 \circ f_{[0;\bar{3}]}^0$ (consider equation (4) and the flow diagram). Each of these effective maps can be considered as a dynamical system with fixed points and periodic orbits of different lengths.

Now two natural questions arise: Which cycle of the renormalization flow does lead to the minimal (respectively maximal) local scaling exponent? Which fixed point or periodic orbit of the dynamical system corresponding to this cycle does yield the extremal scaling exponent? In a first step, these two questions can be addressed numerically by determining the index of the band of maximal (respectively minimal) width and following its way under the renormalization flow.

We find that the the minimal scaling exponent for $\omega = [0; \bar{n}]$ occurs for the cycle R (these ω are fixed points of R), i.e. the smallest bands occur at the edges of the spectrum. More interestingly, the maximal scaling exponent occurs for the cycle $S^{n-1}R$ (n odd) respectively for $S^{\frac{n}{2}-1}R$ (n even). The lengths and the structure of these cycles show a striking even-odd effect which is a direct result of the Hofstadter rules. Furthermore, for n odd the maximal scaling exponent is given by the fixed point of the effective dynamical system, while for even values of n the asymmetric orbit of length two yields the maximal scaling exponent.

For the minimal exponent we find for $\omega = [0; \bar{n}]$:

$$\alpha_{\min} = -\frac{\ln \tilde{\omega}}{\ln z_R([0; \bar{n}])} \quad (14)$$

and for the maximal exponent we obtain

$$\alpha_{\max} = -\frac{2 \ln \tilde{\omega}}{\ln |f_{\text{eff}}^{\pm'}(E_1^*)|} \quad \text{if } n \text{ odd} \quad (15)$$

$$\alpha_{\max} = -\frac{\ln \tilde{\omega}}{\ln |f_{\text{eff}}^{\pm'}(E_2^*)|} \quad \text{if } n \text{ even} \quad (16)$$

where E_1^* (E_2^*) is the energy of the fixed point (energy of the orbit of period two) of the effective map $f_{\text{eff}}^{\pm}(E)$. Replacing the effective map $f_{\text{eff}}^{\pm}(E)$ by the individual maps, we find

$$\alpha_{\max} = -\frac{2 \ln \tilde{\omega}}{\sum_{i=1, i \neq 2}^n \ln z_S([0; i, \bar{n}]) + \ln z_R([0; 2, \bar{n}])} \quad \text{if } n \text{ odd} \quad (17)$$

$$\alpha_{\max} = -\frac{\ln \tilde{\omega}}{\sum_{i=4, i \text{ even}}^n \ln z_S([0; i, \bar{n}]) + \ln z_{R_{\pm}}([0; 2, \bar{n}])} \quad \text{if } n \text{ even.} \quad (18)$$

Inspecting these two equations one is lead to the assumption that α^{\max} as a function of $\omega = [0; \bar{n}]$ should be sensible to the parity of n , while α_{\min} is expected to show a monotonic behaviour as a function of n . This is indeed the case, as shown in figure 6. For a more quantitative discussion of our approximation, however, the behaviour of z_R , $z_{R_{\pm}}$ and z_S as a function of ω is required. For limiting cases, as $\omega \rightarrow 0$ or $\omega \rightarrow \frac{1}{2}$, the contraction factor z_S can be obtained by semiclassical analysis and by considering tunnelling in phase space [28, 29, 5, 30–32], if one makes the further assumption that $f_{\omega}^0(E)$ is nearly linear, so that z_S can be written as ratio of band edges: $z_S(\omega) = E_{1-}(\omega)/E_0(S(\omega))$. For $\omega \rightarrow 0$ $z_S(\omega)$ is therefore given by the ratio of two Landau levels and with the results of [5] we find:

$$z_S(\omega) = 1 - \pi\omega + \pi\omega^2 + \left(2\pi - \pi^2 + \frac{\pi^3}{24}\right)\omega^3 + \mathcal{O}(\omega^4) \quad (\omega \rightarrow 0). \quad (19)$$

For $\omega \rightarrow \frac{1}{2}$ tunnelling has to be taken into account for determining $E_{1-}(\omega)$ and we find

$$-\frac{1}{\ln z_S(\omega)} \simeq b_S(\frac{1}{2} - \omega) + c_S(\frac{1}{2} - \omega)^2 + d_S(\frac{1}{2} - \omega)^2 \ln(\frac{1}{2} - \omega) \quad (\omega \rightarrow \frac{1}{2}) \quad (20)$$

where b_S is given analytically by $b_S = \pi(\int_0^{\pi/2} \ln(\cos k + \sqrt{1 + \cos^2 k}) dk)^{-1} \approx 3.429 815$ and c_S and d_S are fit parameters (cf appendix). Although equations (19) and (20) are only expansions near $\omega = 0$ and $\omega = \frac{1}{2}$, they describe $z_S(\omega)$ over the whole range $0 < \omega < \frac{1}{2}$ amazingly well, if one takes equation (19) for $0 < \omega < 0.25$ and equation (20) for $0.25 < \omega < 0.5$ (cf figure 5). In principle, a similar analysis can be performed for the mean slope $\bar{z}_R = (E_0(\omega) - E_{1+}(\omega))/(2E_0(R(\omega)))$. As the linear approximation for $f^{\pm}(E)$ assumed in this relation is a rather crude one for general ω , the values of z_R and $z_{R_{\pm}}$ can deviate considerably from \bar{z}_R . This, however, is not the case for $\omega \rightarrow 0$, where z_R and $z_{R_{\pm}}$ are well approximated by \bar{z}_R that is given in this regime by

$$-\frac{1}{\ln \bar{z}_R(\omega)} = b_R\omega + c_R\omega^2 + d_R\omega^2 \ln \omega \quad (\omega \rightarrow 0) \quad (21)$$

where $b_R = 2\pi(\int_0^{2\pi} \ln(2 - \cos k + \sqrt{(2 - \cos k)^2 - 1}) dk)^{-1} \approx 0.857 454$ and $c_R \approx 1.5$ and $d_R \approx 0.37$ again are fit parameters.

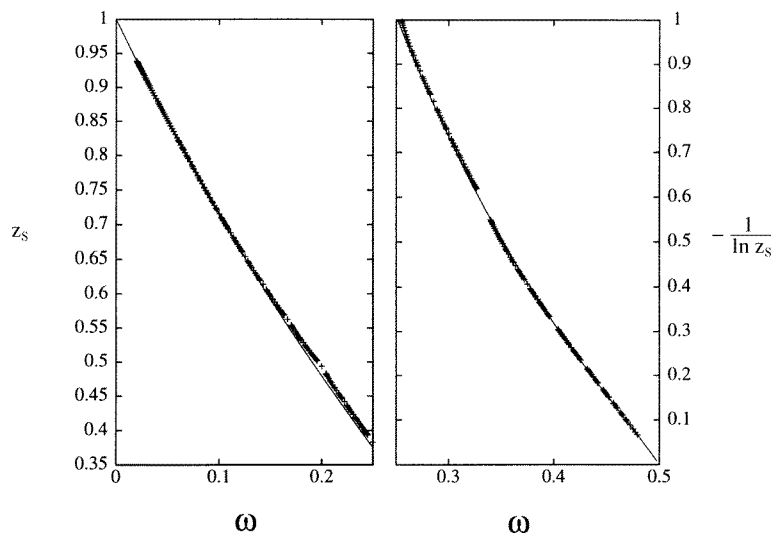


Figure 5. The contraction factor $z_S(\omega) = E_{1-}(\omega)/E_0(\omega)$ compared to the results from semiclassical analysis (equation (19) for $0 < \omega < 0.25$ and equation (20) for $0.25 < \omega < 0.5$ ($b_S = 3.429815$, $c_S = 9.6$, $d_S = 5.2$)). Note that $z_S(\omega)$ is remarkably smooth compared to $E_{1-}(\omega)$ and $E_0(\omega)$ (figure 3).

As α_{\min} is determined by $z_R[0; \bar{n}] \approx \bar{z}_R[0; \bar{n}]$ (as $[0; \bar{n}] \rightarrow 0$ for $n \rightarrow \infty$), we insert equation (21) into (14) and obtain

$$\alpha_{\min} \simeq (b_R \omega + c_R \omega^2 + d_R \omega^2 \ln \omega) \ln \tilde{\omega} \quad (22)$$

where $\omega = \frac{1}{2}(\sqrt{n^2 + 4} - n)$ and $\tilde{\omega} = \frac{1}{2}(n + \sqrt{n^2 + 4})$. Therefore, asymptotically $\alpha_{\min} \sim b_R \ln n/n$ ($n \rightarrow \infty$) and $\lim_{n \rightarrow \infty} \alpha_{\min} = 0$.

For α^{\max} the values z_R and $z_{R_{\pm}}$ for ω near to $\frac{1}{2}$ are needed. As they are not directly available in our approach, we take approximately $z_R(\omega) = \bar{z}_R(\omega)$ and $z_{R_{\pm}} = 1.4\bar{z}_R(\omega)$, where $\bar{z}_R(\omega)$ is given by equation (21). This approximation is intended to give the qualitative behaviour for α^{\max} .

In figure 6 the predictions for α_{\min} and α^{\max} for $3 \leq n \leq 10$ are compared with the corresponding values obtained by diagonalization. For α_{\min} and $n \geq 5$ there is good agreement between prediction and simulation, while for $n < 5$ the predicted value of α_{\min} is too high, reflecting the fact that $z_R < \bar{z}_R$. For α^{\max} we find qualitatively the even-odd oscillations, but of course, due to the problems mentioned above, we cannot hope to achieve quantitative agreement. In particular an open question is the behaviour of α^{\max} for $n \rightarrow \infty$. For the moment, we can only state, that if $\ln z_R(\omega)$ and $\ln z_{R_{\pm}}(\omega)$ is bounded for $\omega \rightarrow \frac{1}{2}$, then α^{\max} does not reach the value 1 for $n \rightarrow \infty$.

4. Conclusion

We have used a refined version of Hofstadter rules together with results from semiclassical analysis to link the maximal and minimal fractal dimension of the spectrum of the Harper equation to the continued-fraction expansion of the irrational number characterizing the flux per unit-cell. We have shown that the oscillatory behaviour of α^{\max} for $\omega = [0; \bar{n}]$ as a function of n can be qualitatively explained by the discrete flow diagrams of the Hofstadter

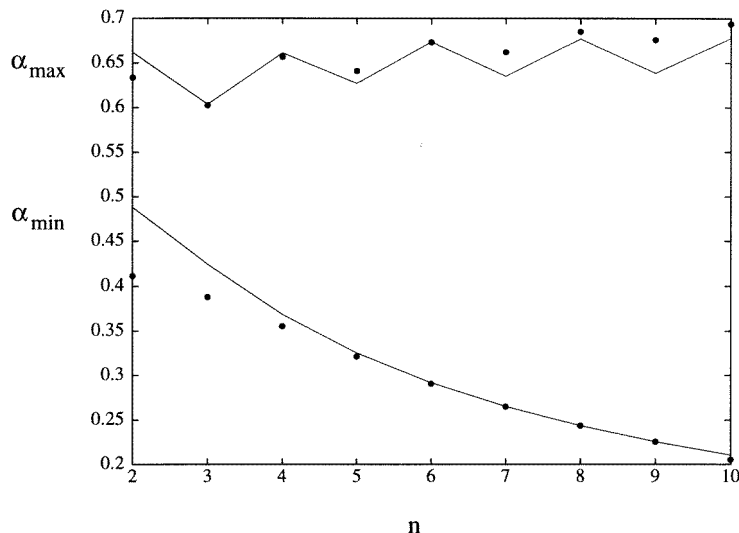


Figure 6. The fractal dimensions $D_{-\infty} = \alpha_{\max}$ and $D_{\infty} = \alpha_{\min}$ for $\omega = [0; \bar{n}]$ as a function of n . Results of diagonalization are depicted with points, the lines refer to equations (22) and (18)

rules. For α_{\min} an explicit expression has been given which describes fairly well the data obtained by diagonalization. We conjecture that the result for α_{\max} can be generalized to quadratic numbers of the continued fraction expansion $\omega = [0; \bar{n}_1, n_2, \dots, n_p]$. Take for example $\omega = [0; \bar{n}_1 n_2]$: In this case the renormalization flow diagram contains $\frac{1}{2}(n_1 + n_2)$ different irrational numbers, if both n_1 and n_2 are even. In all the other cases, there are $n_1 + n_2$ different irrational numbers. Thus, for even values of n_1 the cycle structure depends on the parity of n_2 , while this is not the case for n_1 odd. Hence, for fixed even values of n_1 we expect even-odd oscillations of α_{\max} as function of n_2 , while for odd values of n_1 no such oscillations are expected.

Finally we note that the applicability of the Hofstadter rules to a wide class of quasiperiodic models suggests that our method could be useful for other models than the one we have considered here.

Appendix

This appendix is intended to provide the calculations for z_S and \bar{z}_R in the semiclassical approximation using methods and results described in [29, 5, 30–32].

Equation (19) can be obtained directly by inserting the semiclassical expansion of the Landau levels up to order three [5] into

$$z_S(\omega) = \frac{E_{1-}(\omega)}{E_0(\frac{\omega}{1-2\omega})} \quad (\omega \rightarrow 0). \quad (23)$$

For $\omega \rightarrow \frac{1}{2}$ the contraction factor z_S is given by

$$z_S(\omega) = \frac{E_{1-}(\omega)}{E_0(4(\frac{1}{2}\omega))} \quad (\omega \rightarrow \frac{1}{2}). \quad (24)$$

While the denominator corresponds to Landau levels near $\omega = 0$ and the already mentioned semiclassical expansion can be used, the numerator involves the calculation of $E_{1-}(\omega)$ for

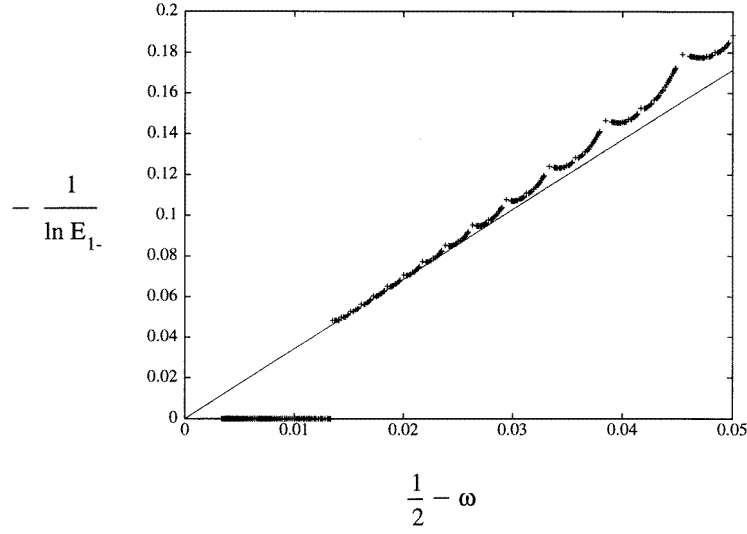


Figure 7. The broadening of the Dirac level at $E = 0$, $\omega = \frac{1}{2}$ compared to the result from tunnelling in phase space $-1/\ln E_{1-}(\omega) \sim 2\pi(\frac{1}{2} - \omega)/|\text{Im } S|$, where the imaginary part of the action is given by $|\text{Im } S| = \int_{-\pi/2}^{\pi/2} \ln(\cos k + \sqrt{1 + \cos^2 k}) dk \approx 1.831931$. For $\frac{1}{2} - \omega < 0.013$ the broadening of Dirac levels cannot be resolved numerically.

$\omega \rightarrow \frac{1}{2}$. Since for $\omega = \frac{1}{2}$ the effective Hamiltonian $H = \pm 2\sqrt{\cos^2 k_1 + \cos^2 k_2}$ has the form of a Dirac operator at the four critical points $(\pm\frac{\pi}{2}, \pm\frac{\pi}{2})$ (independent signs) [5], we are left with the calculation of tunnelling between Dirac levels.

Although the usual formula for level splitting due to tunnelling

$$\Delta E \sim \text{constant} \times \hbar \exp\left(-\frac{|\text{Im } S|}{\hbar}\right) \quad (25)$$

where S is the action integral between degenerate minima, \hbar is Planck's constant and the proportional constant is related to the classical frequency, was originally derived for tunnelling between parabolic minima [33], we tentatively use it for our case, where the minima are conical. With $\hbar = 2\pi(\frac{1}{2} - \omega)$ [5] we obtain

$$E_{1-}(\omega) \sim (\frac{1}{2} - \omega) \exp\left(-\frac{|\text{Im } S|}{2\pi(\frac{1}{2} - \omega)}\right) \quad (26)$$

where the action integral has to be calculated between two adjacent minima in phase space. The (complex) orbits are given by $H = 0$, i.e. $\cos^2 k_1 + \cos^2 k_2 = 0$ and therefore

$$S = \int_{-\pi/2}^{\pi/2} \arccos(\pm i \cos k_1) dk_1 \quad (27)$$

$$|\text{Im } S| = 2 \int_0^{\pi/2} \ln(\cos k_1 + \sqrt{1 + \cos^2 k_1}) dk_1 \approx 1.831931. \quad (28)$$

Formula (26) with (28) inserted is compared to numerical results from diagonalization in figure 7. We note that the fact of the action being purely imaginary shows the absence of braiding of the Dirac levels. To calculate $z_S(\omega \rightarrow \frac{1}{2})$ we insert (26) together with

$$E_0(4(\frac{1}{2} - \omega)) \sim 4 - 8\pi(\frac{1}{2} - \omega) + \mathcal{O}((\frac{1}{2} - \omega)^2) \quad (29)$$

into (24) and obtain (20). The parameters $c_S \approx 9.6$ and $d_S \approx 5.2$ are determined by fitting to the numerical data.

The calculations for $\overline{z}_R(\omega \rightarrow 0)$ are analogous, but only Landau levels have to be considered.

References

- [1] Harper P G 1955 *Proc. R. Soc. A* **68** 874
- [2] Thouless D J, Kohmoto M, Nightingale P and den Nijs M 1982 *Phys. Rev. Lett.* **49** 405
- [3] Pannetier B, Chaussy J, Rammal R and Villegier J C 1984 *Phys. Rev. Lett.* **53** 1845
- [4] Gerhardt R, Weiss D and Wulf U 1991 *Phys. Rev. B* **43** 5192
- [5] Rammal R and Bellissard J 1990 *J. Physique* **51** 1803
- [6] Bellissard J 1987 *Operator Algebras and Applications* vol 2, ed D E Evans and M Takesaki (Cambridge: Cambridge University Press)
- [7] Wiegmann P B and Zabrodin A V 1994 *Phys. Rev. Lett.* **72** 1890
- [8] Schlösser T, Ensslin K, Kotthaus J P and Holland M 1996 *Europhys. Lett.* **33** 683
- [9] Halsey T S, Jensen M H, Kadanoff L P and Shraiman B I 1986 *Phys. Rev. A* **33** 1141
- [10] Kohmoto M and Oono Y 1984 *Phys. Lett.* **102A** 145
- [11] Tang C and Kohmoto M 1986 *Phys. Rev. B* **34** 2041
- [12] Kohmoto M, Sutherland B and Tang C 1987 *Phys. Rev. B* **35** 1020
- [13] Zheng W M 1987 *Phys. Rev. A* **35** 1467
- [14] Hiramoto H and Kohmoto M 1992 *Int. J. Mod. Phys.* **6** 281
- [15] Ikezawa K and Kohmoto M 1994 *J. Phys. Soc. Japan* **63** 2261
- [16] Piéchon F, Benakli M and Jagannathan A 1995 *Phys. Rev. Lett.* **74** 5248
- [17] Rüdinger A and Sire C 1996 *J. Phys. A: Math. Gen.* **29** 3537
- [18] Bell S C and Stinchcombe R B 1989 *J. Phys. A: Math. Gen.* **22** 717
- [19] Thouless D J 1983 *Phys. Rev. B* **28** 4272
- [20] Last Y and Wilkinson M 1992 *J. Phys. A: Math. Gen.* **25** 6123
- [21] Tan Y 1995 *J. Phys. A: Math. Gen.* **28** 4163
- [22] Wilkinson M and Austin E J 1994 *Phys. Rev. B* **50** 1420
- [23] Piéchon F 1996 *Phys. Rev. Lett.* **76** 4372
- [24] Holzer M 1988 *Phys. Rev. B* **38** 1709
- [25] Holzer M 1988 *Phys. Rev. B* **38** 5756
- [26] Hofstadter D R 1976 *Phys. Rev. B* **14** 2239
- [27] Piéchon F 1995 *PhD Thesis* (Paris)
- [28] Wilkinson M 1987 *J. Phys. A: Math. Gen.* **20** 4337
- [29] Wilkinson M and Austin E J 1990 *J. Phys. A: Math. Gen.* **23** 2529
- [30] Barelli A and Kreft C 1991 *J. Physique I* **1** 1229
- [31] Barelli A and Fleckinger R 1992 *Phys. Rev. B* **46** 11 559
- [32] Bellissard J and Barelli A 1993 *J. Physique I* **3** 471
- [33] Landau L D and Lifshitz E M 1955 *Quantum Mechanics* (Oxford: Pergamon)